A NEW FEATURE FOR AUTOMATIC ANEURYSM DETECTION

Clemens M. Hentschke, Klaus D. Tönnies

University of Magdeburg
Department of Simulation and Graphics
Magdeburg, Germany

Oliver Beuing, Rosa Nickl

University Hospital of Magdeburg
Institute for Neuroradiology
Magdeburg, Germany

ABSTRACT

We propose a new feature that can be used to automatically detect cerebral aneurysms in angiographic images. It combines both low-level and high-level features to a feature indicating aneurysms. The feature is used in a system for aneurysm detection in two types of magnetic resonance angiography (MRA) images and computed tomography angiography (CTA) images. The method was tested on 66 angiographic data sets containing aneurysm and non-aneurysm cases. We show that the newly introduced incorporation of the location based feature improves the detection quality. We achieve a sensitivity higher than 93 % for all modalities with an average false positive rate varying from 8.8 to 20.9 per data set, depending on the modality.

Index Terms— Aneurysm, Computer aided Diagnosis, Object detection, Angiography.

1. INTRODUCTION

Approximately 3 % of the population harbors one or more cerebral aneurysms [1]. Cerebral aneurysms can lead to rupture that causes a life-threatening subarachnoid hemorrhage. The mortality rate for this pathology is reported to be approximately 50 %, while 46 % of the survivors have long-time impairments. Rupture of aneurysms has to be prevented with respect to clinical and economical aspects. Hence, early finding of cerebral aneurysms is desirable as a prognosis if and when an aneurysm ruptures is currently not possible with sufficient accuracy [2].

Three-dimensional image modalities that are clinically relevant in aneurysm detection are 3D X-ray rotational angiography (3D-RA), Time-of-Flight magnetic resonance angiography (TOF-MRA), Contrast-Enhanced MRA (CE-MRA) and computed tomography angiography (CTA). As TOF-MRA is non-invasive and CE-MRA and CTA are minimally invasive and depict the whole cerebral vasculature rather than 3D-RA, we focus on these modalities.

Aneurysms are commonly found incidentally and typically remain asymptomatic until their rupture. Computer-aided diagnosis (CAD) assists the radiologist to find pathologies in medical images. CAD can be used in this case to prepare angiographic data highlighting aneurysms. Generally, CAD techniques are based on feature computation and analysis. First, initial volumes of interest (VOI) are found by generalizing image-based characteristics of the abnormality. These VOI include true positives (TP) and false positives (FP). A classification step discriminates between these classes.

Few algorithms have been published to detect cerebral aneurysms in medical images [3, 4, 5]. Only one algorithm was tested with multi-modal images [4]. No algorithm was tested with CTA without bone subtraction or CE-MRA. For example, gray level features have been used in a linear discriminant analysis [3]. As most of the proposed algorithms rely on a statistical analysis, a sufficiently large and representative database is necessary to ensure generality. Otherwise, the algorithm may adapt to the specific characteristics of a database biased by different scanners, ethnicities or disease patterns.

We aim to construct a feature that can be used for classification without training of a discriminant function. This is done by combining low-level and high-level image-derived features. Model-based knowledge about the characteristics of cerebral aneurysms substitutes the training database. More precisely, we use gray-level, morphological and location-based features, the latter not having been used before in the context of aneurysm detection. The proposed combined feature can be adopted for different angiographic modalities using a small number of parameters.

2. METHOD

The proposed method aims at finding cerebral aneurysms in multi-modality angiographic data sets. A generalization of aneurysms with respect to shape or gray-level distributions is difficult. Aneurysms can be saccular or fusiform, which implies a rather different shape. Furthermore, the different modalities lead to different characteristics. The more information about brain matter or skull is present in data, the more challenging is the detection task. CTA without bone-subtraction is the most challenging modality as bone matter and blood vessels overlap in their Hounsfield Unit (HU) values.

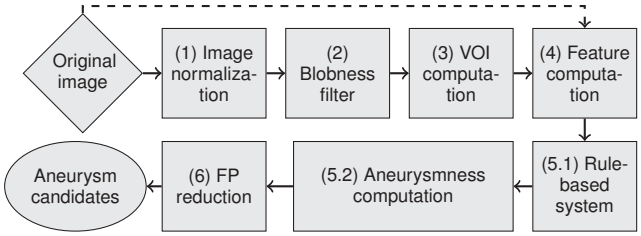


Fig. 1. The scheme of the proposed algorithm.

An overview of our scheme is given in Fig. 1. First, the data sets are normalized. The data sets are then processed by a sphere-enhancing filter. VOI are found by applying a connected-component analysis (CCA). Several low-level and high-level features are computed for each VOI. A rule-based system (RBS) excludes FP based on simple rules. The new feature *aneurysmness* is then derived. The VOI having the highest aneurysmness values of a data set are taken as final aneurysm candidates.

In order to cope with different modalities, we use a parametrizable scheme that is adapted according to the modality. The parametrization is given in Table 1. The processing of CE-MRA and TOF-MRA differs only in detail.

The image normalization (step 1) consists of a contrast stretching, an orienation normalization and an isotropic voxel resampling. In CTA, the gray levels are already normalized due to HU values. This has the advantage that the intensity level of vessel voxels is known and can be used as a mask for the subsequent filter computation in CTA.

In step 2, a multi-scale-filter enhances spherical structures (blobness) in the normalized data set. The filter is a generalization of the vesselness filter [6]. In step 3, a CCA is applied to the binary-segmented image with threshold t to exclude poorly enhanced regions from initial VOI candidates. See Table 1 for parametrization of t.

Overall, 13 distinct features are computed on the VOI (step 4). These are:

- i_{avg}, i_{min}, i_{max}: intensity (average (avg), minimal (min) and maximal (max) value),
- b_{avg}, b_{min}, b_{max}: blobness [6] to enhance sphere-like structures with a diameter between 2 mm and 10 mm (Larger structures are found as multiple substructures),
- v_{avg}, v_{min}, v_{max}: vesselness [6], computed based on a typical vessel diameter between 2 mm and 6 mm,
- d_{bx}, d_{by}, d_{bz}: relative distance to the boundary of the image (in x, y and z direction),
- s: volume of the VOI.

In step 5.1, we use a rule-based system (RBS) to exclude FP based on a knowledge-based approach. The parameter settings for the modalities are given in Table 1 and were found experimentally.

Table 1. Parametrization for each step of the workflow and all modalities. The step numbers refer to Fig. 1. I_{max}: maximal intensity of an image, $s(I)$: size of an image.

Step	MRA	CTA
1	$i = [0, 2048]$	$400 > i_{\text{avg}} > 100$
2	The same for all modalities, as described	
3	$t = 0.2 \cdot I_{\text{max}}$	$t = 0.12 \cdot I_{\text{max}}$
4	13 features are computed	
5.1	$400 > i_{\text{avg}} > 100$ $d_{bx} = d_{by} = d_{bz} > 0.2 \cdot s(I)$ $s > 8$ mm^3 $\quad$ $s > 5$ mm^3 0 mm $\leq d_{\text{CoW}} \leq 10$ mm	
5.2	The same for all modalities, see Eq. 1	
6	The same for all modalities, as described	

Together with neuroradiologists, we found different features that correspond to key characteristics of aneurysms: (1) a high blobness indicating a high grade of sphericity, (2) a high vesselness as aneurysms are located in the direct vicinity of vessels, (3) a small distance to the next artery in the Circle of Willis as aneurysms are commonly located there, (4) a large distance to the image boundary as they are located rather medial than lateral and (5) a minimal diameter of 2 mm. Additionally, we identified a large volume of the VOI as useful feature. The characteristic features are used in our proposed feature aneurysmness, the other features are used for evaluation purposes.

The feature aneurysmness (step 5.2) is defined as follows:

$$A = w_1\bar{b} + w_2\bar{v} + w_3\bar{s} + w_4\bar{d}_b + w_5\bar{d}_{\text{CoW}}, \qquad (1)$$

with

$$\bar{b} = \frac{b_{\text{avg}}}{\max b_{\text{avg}}},\ \bar{v} = \frac{v_{\text{avg}}}{\max v_{\text{avg}}},$$
$$\bar{d}_{\text{CoW}} = 1 - \frac{d_{\text{CoW}}}{\max d_{\text{CoW}}},\ \bar{d}_b = \frac{d_{bx} + b_{by} + d_{bz}}{3 \cdot \max d_b},$$
$$\bar{s} = \frac{s}{\max s},\ d_b = \min\left(\frac{p}{s(I)}, \frac{s(I) - p}{s(I)}\right),$$
$$\sum_{i=1}^{5} w_i = 1 \text{ and } 0 \leq w_i \leq 1,\ \ i = 1, \ldots, 5.$$

In this Equation, d_{CoW} is the distance of the VOI center to the next Circle of Willis artery and is a newly introduced feature. p is the coordinate value, $s(I)$ is the image size. $\max d_{CoW} = 20$ mm and $\max d_b = 0.5$ are constants. Note that $\max$ is computed for each data set individually.

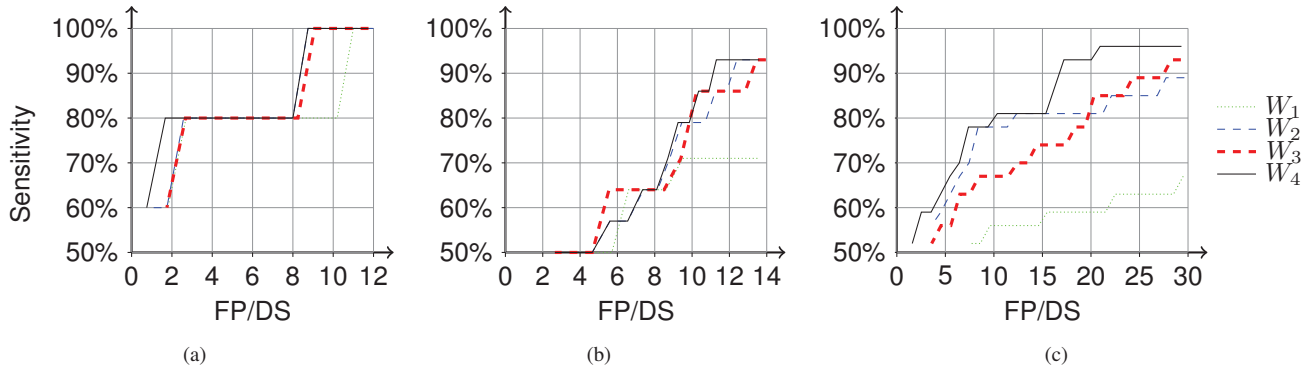


Fig. 2. The FROC for experiment 1 for (a) CE-MRA, (b) TOF-MRA and (c) CTA. Note that the x-axes are scaled differently.

d_b and s are low-level features that can be directly computed based on VOI properties. b, v and d_{CoW} are high-level features that require pre-computation and include model-based knowledge. Gray level information, morphological information and location information are integrated in the aneurysmness feature.

Our system shall not require a vessel segmentation as it heavily influences the detection quality [4] while in the case of CTA without bone-subtraction, vessel segmentation is not known at all.

Since inclusion of the vessel information is advantageous nonetheless, we propose an atlas-based registration to classify voxels as background or vessel. This is included by d_{CoW} into the aneurysmness feature. We manually determined a model data set for CE-MRA, TOF-MRA and CTA. In case of the MRA modalities, the model consists of a manually corrected threshold-based segmentation of the Circle of Willis arteries. In case of the CTA model, a manually segmented CE-MRA data set of the same patient was registered to the CTA data set. Then, a distance-transform is applied to the segmented model data sets with a maximum distance of 20 voxels (approximately 10 mm). The original model data set is then registered to each data set using a rigid multi-scale registration with normalized cross correlation as similarity metric. The registration is done with the elastix toolkit [7]. The distance of a VOI to the next vessel of the Circle of Willis arteries, d_{CoW} can be determined by a lookup in the registered distance-transformed model data set. Background has a value of $d_{CoW} < 0$. In our experiments, the registration aligns the model well to the data. By using the distance transform, we account for registration errors and inter-patient variance.

The aneurysmness feature A is defined in the range of $[0, 1]$ with 1 meaning the highest probability of a VOI to be aneurysm. We order the VOI based on their A values on each data set individually (step 6). Thus, we apply a thresholding on the order of A, i.e. the n highest A values are taken as final aneurysm candidates. Although we applied an image normalization, the aneurysmness intra-data set comparability is still better than the inter-data set comparability.

3. RESULTS

We tested our system on 32 clinical MRA data sets (20 TOF-MRA, 12 CE-MRA) and on 34 clinical CTA data sets from different manufacturers. The 66 data sets contain 46 aneurysms with 31 data sets incorporating no aneurysms. The diameter of the aneurysms vary between 1.5 mm and 32 mm. The ground truth (number and location of aneurysms) was given by a neuroradiologist who had access to the clinical report.

We tested different parameterizations of the aneurysmness feature to evaluate the quality gain of the detection system through the addition of location features. The weightings are defined as $W = \{w_1, w_2, w_3, w_4, w_5\}$. Additionally, we compared the quality of the aneurysmness feature against all computed features. Two different quality measures are computed: the area under curve (AUC) of the free receiver-operation characteristic (FROC) and the average false positive rate per data set (FP/DS) at a sensitivity of 95 % ($\text{FP}_{0.95}$). As we used a FROC with no absolute specificity, we computed the AUC values based for MRA at a maximal rate of 15 FP/DS and for CTA at a maximal rate of 30 FP/DS as these were plausible maximum FP values. A VOI is rated as TP if the volume overlaps with the expert location mark.

In a first experiment, we determined the influence of the location-based features d_{CoW} and d_b to the detection quality. The weighting and the RBS (step 5.1 and step 5.2) had to be changed. We used the following weighting set for Eq. 1: $W_1 = \{0.33, 0.33, 0.33, 0, 0\}$ and no rules in the RBS, $W_2 = \{0.25, 0.25, 0.25, 0.25, 0\}$ and the d_{CoW} rule not applied in the RBS, $W_3 = \{0.25, 0.25, 0.25, 0, 0.25\}$ and the d_b rules not applied in the RBS and $W_4 = \{0.2, 0.2, 0.2, 0.2, 0.2\}$ with all rules of the RBS system applied.

The results are shown in Fig. 2. The addition of the location information improves the algorithm considerably independent of the modality. The parametrization W_4 including all information yields to the best results in TOF-MRA and CTA. Not all modalities benefit equally from the new features. In the case of CE-MRA, the AUC value rises from $W_1 = 0.79$

Table 2. Results of experiment 2. The best values for each column are printed bold. The 4 features i_{avg}, b_{min}, v_{min} and v_{max} leading to the worst AUC values are not shown.

	CE-MRA		TOF-MRA		CTA	
feat.	**AUC**	**FP**$_{0.95}$	**AUC**	**FP**$_{0.95}$	**AUC**	**FP**$_{0.95}$
s	**0.89**	**5.3**	0.64	11.7	0.64	40.3
i_{min}	0.57	15.4	**0.77**	**7.4**	0.36	73.6
i_{max}	0.70	8.8	0.43	11.3	0.2	89.0
b_{avg}	0.70	11.8	0.61	11.3	0.71	35.9
b_{max}	0.82	6.3	0.61	11.3	0.69	38.9
v_{avg}	0.69	11.1	0.54	11.3	0.69	83.6
A	0.83	9.6	0.62	11.3	**0.81**	**20.9**

to $W_4 = 0.86$, in TOF-MRA, the value increases from 0.57 to 0.62 and in CTA, the value increases clearly from 0.53 to 0.81. This shows that d_{CoW} and d_b are useful additional information for distinguishing VOI between FP and aneurysms. Best results are achieved if both features are used.

In a second experiment, we tested the quality of the aneurysmness feature against all initially referred features. We used the parametrization W_4 that produced the best results. The results are shown in Table 2 and differ depending on the modality. In CE-MRA and TOF-MRA, single features lead to better results than the aneurysmness feature. In case of CTA, the aneurysmness is the feature leading to the best results. These results are according to our expectations. We wanted to test the new feature with the same parametrization for all three modalities, what did not lead to the best possible results in the MRA modalities.

An adapted parametrization by fortify the weighting of discriminatory features leads to considerably better results by exploiting the modality-specific characteristics. For example, we measured an AUC value of 0.79 (93 % sensitivity at 6.3 FP/DS) for TOF-MRA. The weighting setting is subject for further research. The aneurysmness feature consisting of a subset of all features leads to better results if the location information has a high significance. This is the case especially in CTA.

Overall, using the proposed aneurysmness feature we reach a sensitivity of 100 % at 8.75 FP/DS in case of CE-MRA and 93 % sensitivity at 11.3 FP/DS for TOF-MRA. We reach a similar quality than [5] who defined a rule-based system with experimentally found rules. A sensitivity of 96 % at 11.6 FP/DS was reported. However, we do neither require expert-set rules, nor a characteristic training database.

In case of CTA, we reach a sensitivity of 96.3 % at 20.94 FP/DS. Compared to our previous publication [8], FP$_{0.95}$ dropped from 37.6 to 20.9. The only other algorithm that works on CTA data sets has reported a sensitivity of 100 % at 5.4 FP/DS [4]. However, this method requires bone-subtracted CTA and was only tested on 10 data sets. All similar algorithms require a segmentation of the vasculature.

4. CONCLUSIONS

We proposed a feature for automatic cerebral aneurysm detection. The feature is used in a CAD system and it combines low-level features and high-level features to establish the challenging generalization of an aneurysm. An adaptation for several angiographic modalities is possible through the parametrization. The aneurysmness is easily extendable to include other features.

The whole CAD-system consists of a workflow that can be parametrized for three modalities: CE-MRA, TOF-MRA and CTA without bone subtraction. First, the original image is processed by a sphere-enhancing filter. Initial VOI are found by a CCA on the filtered image. The aneurysmness and a RBS are then used to eliminate FP without reducing the sensitivity.

For the future, we want to further reduce the amount of FP by incorporating additional location-dependent information. We believe that our system could also be used to detect similar diseases like lung nodules in CT images.

5. REFERENCES

[1] M.H. Vlak, A. Algra, R. Brandenburg, and G.J. Rinkel, "Prevalence of unruptured intracranial aneurysms, with emphasis on sex, age, comorbidity, country, and time period: a systematic review and meta-analysis," *Lancet neurology*, vol. 10, no. 7, pp. 626–636, 2011.

[2] J. van Gijn, R.S. Kerr, and G.J. Rinkel, "Subarachnoid haemorrhage," *Lancet*, vol. 369, no. 9558, pp. 306–18, 2007.

[3] H. Arimura, Q. Li, Y. Korogi, T. Hirai, S. Katsuragawa, Y. Yamashita, K. Tsuchiya, and K. Doi, "Computerized detection of intracranial aneurysms for three-dimensional MR angiography," *Medical Physics*, vol. 33, no. 2, pp. 394, 2006.

[4] A. Lauric, E. Miller, S. Frisken, and A.M. Malek, "Automated detection of intracranial aneurysms based on parent vessel 3D analysis," *Medical Image Analysis*, vol. 14, no. 2, pp. 149–159, 2010.

[5] X. Yang, D.J. Blezek, L.T. Cheng, W.J. Ryan, D.F. Kallmes, and B.J. Erickson, "Computer-Aided Detection of Intracranial Aneurysms in MR Angiography," *Journal of Digital Imaging*, vol. 24, no. 1, pp. 86–95, 2011.

[6] A.F. Frangi, W.J. Niessen, K.L. Vincken, and M.A. Viergever, "Multiscale vessel enhancement filtering," in *Medical Image Computing and Computer-Assisted Intervention*, 1998, pp. 130–137.

[7] S. Klein, M. Staring, K. Murphy, M.A. Viergever, and J.P. Pluim, "Elastix: a Toolbox for Intensity-Based Medical Image Registration," *IEEE transactions on medical imaging*, vol. 29, no. 1, pp. 196–205, 2010.

[8] C.M. Hentschke, O. Beuing, R. Nickl, and K.D. Tönnies, "Detection of cerebral aneurysms in MRA, CTA and 3D-RA data sets," in *SPIE Medical Imaging, to appear*, 2012.